

Supplementary material to AICC2012 Common for Bazin et al. (2012) and Veres et al. (2012)

The method for the building of AICC2012 is an improved version of Datice presented in Lemieux-Dudon et al. (2010), hereafter LD2010, for 4 ice cores (Vostok, EPICA Dome C, EPICA Dronning Maud Land, NorthGRIP) and modified for TALDICE by Buiron et al. (2011). The aim is to combine chronological information from data and model to build coherent and precise timescales with associated estimates of uncertainty range. For this, the Datice tool needs several inputs. First, independent background scenarios for thinning, accumulation rate and lock-in depth in ice equivalent (LIDIE) have to be implemented for each of the 5 ice cores. Then, Datice builds a correction function associated with each scenario (thinning, accumulation rate, LIDIE). The correction function is more or less allowed to modify the initial scenario depending on the variance associated with each scenario for each ice core. The variance scenarios need to be prescribed by the user. Then, Datice incorporates markers from ice core records such as absolute or orbital age markers on each ice core, gas and ice stratigraphic links between the ice cores and constraints for Δ depth (depth difference between the signatures of the same event in the ice and gas phases). The error statistics of the background and observations must be decorrelated for a proper application of the Datice inverse method. An important aspect of the Datice initialisation that was not modified in this study deeper than in LD2010 is the correlation length that imposes the depth range of the ice core on which a marker influences the correction function. If the correlation length is large, a marker has the effect of modifying on a large depth range the correction function. Finally, Datice calculates a cost function that measures the distance between background scenarios and new scenarios as well as between new scenarios and data constraints. A too high cost function obviously means that there are incoherencies between the inputs proposed by the user.

In the previous studies, the dating method was optimized for the last 50 ka and here we have extended it over the past 800 ka. Several improvements have been made compared to the study of Lemieux-Dudon et al. (2010), both in some background scenarios and in the parameterization of the variance associated with these scenarios. In addition, our new chronology also incorporates numerous new stratigraphic, absolute and orbital markers that strongly reduce the dating uncertainty especially for the last glacial cycle. We provide below all the necessary information and input parameters to run

the open source Datice tool and obtain the AICC2012 chronology for NorthGRIP, Vostok, EDC, EDML and TALDICE. When nothing is specified (i.e. correlation length), then the original LD2010 parameterization is still used.

1 Background parameters

For each ice core, 3 background parameters are needed: accumulation rate, thinning, LIDIE.

1.1 Accumulation rate

For all Antarctic ice cores, we have followed the classical estimate of accumulation rate based on an exponential relationship between accumulation rate and water isotopes (as temperature proxies). For the 4 Antarctic cores, we have thus used exactly the same accumulation rate scenarios as those prescribed in Lemieux-Dudon et al. (2010) and Buiron et al. (2011) (for TALDICE). Note that for Vostok and TALDICE, changes in elevation are taken into account to correct the temperature estimate from the water isotopic profiles. With regard to GICC05, in order to constrain AICC2012 to match GICC05 for the past 60 ka, we have deduced the accumulation rate from the annual layer thickness given by the GICC05modelext (Vinther et al., 2006; Rasmussen et al., 2006; Andersen et al., 2006; Svensson et al., 2008; Wolff et al., 2010) and the strain rate given by the Dansgaard-Johnsen model tuned for NorthGRIP (NorthGRIP Community Members, 2004; Andersen et al., 2006).

1.2 Thinning

For Vostok and EDC, we used the same thinning function as in LD2010. For Vostok, the thinning function is deduced from the accumulation and FGT1 age scale. For EDC, it is deduced from the accumulation and the EDC3 model age scale. Concerning EDML, the thinning function is obtained from the flow model of Huybrechts et al. (2007). Such a background thinning function is different from the one implemented in Lemieux-Dudon et al. (2010) and especially avoids spurious peaks around 500 m depth. We used the same thinning function as Buiron et al. (2011) for TALDICE, obtained from a 1D flow model. For NGRIP, the strain rate is given by the Dansgaard-Johnsen model tuned for NorthGRIP (NorthGRIP Community Members, 2004; Andersen et al., 2006) and used here as thinning background scenario. Note that the background thinning function for NorthGRIP used in Lemieux-Dudon et al. (2010) was not fully consistent with GICC05. As a consequence, there was a slight disagreement between the LD2010 NorthGRIP timescale and GICC05 at the rapid warmings associated with Dansgaard-Oeschger events with differences of ± 30 a. These differences do not exist anymore for AICC2012 (Fig. 4).

1.3 LIDIE

Initially, the background LIDIE for each site came from the Goujon et al. (2003) firnification model (Lemieux-Dudon et al., 2010). The model has been validated over NorthGRIP (Landais et al., 2004; Huber et al., 2006; Guillevic et al., 2012) but seems to overestimate LIDIE for glacial conditions in Antarctic sites except for TALDICE (Landais et al., 2006; Parrenin et al., 2012a; Capron et al., 2012). Parrenin et al. (2012a) have suggested that $\delta^{15}\text{N}$ may provide more realistic constraints on past LID even in low accumulation rate sites. We have thus performed tests with Datice comparing the output LIDIE when using as input the firnification model (background scenario LIDIE 1) and a LIDIE inspired by the $\delta^{15}\text{N}$ profile on each site except NorthGRIP (background scenario LIDIE 2). For this scenario 2, we have assumed that the convective zone did not change over time and took a 0 m convective zone for EDML, TALDICE and EDC and 13 m for Vostok as observed on present firn (Landais et al., 2006; Bender et al., 2006). The LIDIE can then be calculated from the $\delta^{15}\text{N}$ variations in the absence of any rapid temperature variation (2°C in 100 a) at the surface. This condition is valid in Antarctica over the considered period.

$$LIDIE = 0.7 \cdot \delta^{15}\text{N} \cdot R \cdot T / g$$

where T is the mean firn temperature, R the ideal gas constant and g the standard gravity. The factor
60 0.7 stands for the mean density of the firn. A small correction for temperature gradient in the firn
affects the glacial LIDIE in low accumulation rate sites like Vostok and Dome C by 3 m at maxi-
mum. This correction has been taken into account using the firn gradient calculated by the Goujon
et al. (2003) model. For building scenario 2, we have used $\delta^{15}\text{N}$ profiles when they were available
(Dreyfus et al. (2010) for EDC, Sowers et al. (1992) for Vostok, Capron et al. (2012) for TALDICE
65 and EDML). None of these profiles cover the whole depth of the 4 Antarctic ice cores. We then take
advantage of the strong link between $\delta^{15}\text{N}$ and δD evolution on an age scale (Dreyfus et al., 2010).
As a consequence, we could build the missing part of the $\delta^{15}\text{N}$ profiles from the $\delta\text{D}-\delta^{15}\text{N}$ regres-
sion over Terminations using the official ice and gas timescales for each core. Such method has been
applied to fill the gaps of the $\delta^{15}\text{N}$ profiles for EDC over the last 300 ka (except for Terminations
70 where $\delta^{15}\text{N}$ profiles are available, Dreyfus et al. (2010)). For TALDICE, the firnification model has
been shown to be in good agreement with $\delta^{15}\text{N}$ data over the last deglaciation (Capron et al., 2012)
so that we have used the Goujon et al. (2003) LIDIE output to fill the gap over the last interglacial
and last glacial periods.

75 The different background scenarios for LIDIE have a small impact on the final chronology because
the variance associated with the LIDIE background scenario is quite large. As a consequence, the
Antarctic output LIDIE are mostly constrained by the ice and gas stratigraphic points, especially
over the last glacial period where many stratigraphic tie-points are available (see corresponding sec-
tion below). During the last glacial period at EDC, the agreement is better between output and

80 background LIDIE when scenario LIDIE 2 is used (Fig. 1) especially over Termination I. There are several reasons why we do not end with the same LIDIE after analyses at Dome C in LD2010 and in AICC2012. The first reason, which is probably not the more important, is that we have much more stratigraphic points in AICC2012 than in LD2010. The second reason is linked to the background LIDIE scenarios. In AICC2012, the LIDIE background scenario of NorthGRIP is significantly lower
85 than the one in LD2010 (Figure 5 of Veres et al. (2012)). This is due to a better constrained temperature input scenario for the firn densification model used to obtain the background LIDIE of NorthGRIP, in agreement with the full $\delta^{15}\text{N}$ record at NorthGRIP (Landais et al., 2004, 2005; Huber et al., 2006, P. Kindler, pers. comm.) which could not be used in LD2010. For this, we had to use a temporal relationship, $\alpha \sim 0.38$, to link the temperature variations to the ice $\delta^{18}\text{O}$ variations.
90 Similarly, the EDML LIDIE background scenario is smaller in AICC2012 (scenario LIDIE 2) than in LD2010 because it is based on $\delta^{15}\text{N}$ rather than on firnification model. Finally, AICC2012 also incorporates TALDICE background LIDIE scenario given by the firnification model in agreement with the $\delta^{15}\text{N}$ estimate. Then, the numerous gas and/or ice stratigraphic markers, the NorthGRIP, EDML and TALDICE LIDIE are reflected also in the analysed LIDIE for Dome C. As a consequence, if the LIDIE scenarios are smaller at EDML and NorthGRIP in AICC2012 than in LD2010,
95 this will automatically leads to a smaller LIDIE at EDC.

Table 1. Origin of the background parameter profiles

	Accu.	Thinning	LIDIE
Vostok	From isotope	Accu. - FGT1	$\delta^{15}\text{N} - \delta D$
EDC	From isotope	Accu. - EDC3 model	$\delta^{15}\text{N} - \delta D$
EDML	From isotope	Huybrechts et al. (2007)	$\delta^{15}\text{N} - \delta D$
TALDICE	From isotope	1D-flow model (Buiron et al., 2011)	$\delta^{15}\text{N} - \text{firn model}$
NGRIP	From GICC05	From GICC05	Firn model

Finally, it should be noted that the Datiche model can be run with several interpolations from the background scenario, i.e. a fast mode with an interpolation of the background scenario every 2 or 3
100 points or a slow mode with use of the background scenario with its prescribed resolution (1 m for NorthGRIP, 0.55 m for EDC, 1 m from the surface down to 125 m and then 0.5 m below for EDML, 1 m for Vostok and 1 m for TALDICE). Since the initial resolution of the background scenario and the interpolation step may have an influence on the final chronology, we have performed tests with several resolutions. It appears that this effect is negligible compared to the effect of uncertainties
105 associated with the tie-points or the variances associated with the background scenarios which are thus the important parameters to be imposed (see next section).

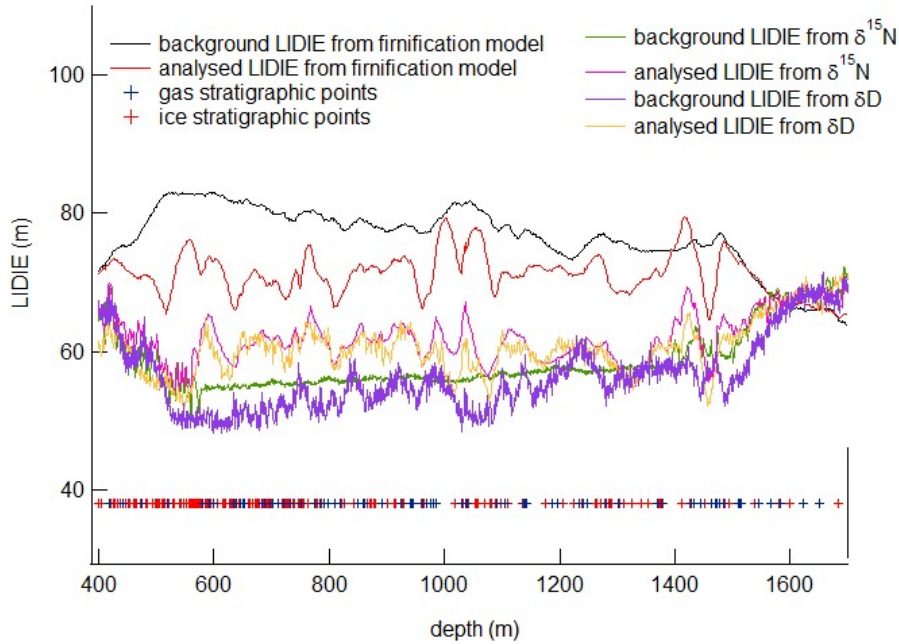


Fig. 1. Different tests on the EDC chronology for the choice of the best LIDIE scenario. Black line: LIDIE background scenario from the firnification model of Goujon et al. (2003). Red line: LIDIE output scenario when Datice is run with background LIDIE from the firnification model. Green line: LIDIE background scenario calculated from $\delta^{15}\text{N}$ values (Dreyfus et al. (2010) over TII; unpublished values for MIS 5). A linear interpolation has been applied between $\delta^{15}\text{N}$ based LIDIE at the beginning and at the end of the the last glacial period to cover the period where no $\delta^{15}\text{N}$ measurements on EDC are available. Pink line: LIDIE output scenario when Datice is run with background LIDIE from $\delta^{15}\text{N}$ data. Purple line: LIDIE background scenario calculated from $\delta^{15}\text{N}-\delta\text{D}$ scenario. It has been observed that for different Antarctic sites, $\delta^{15}\text{N}$ and δD are well correlated on an age scale (Dreyfus et al., 2010; Capron et al., 2012). We use here the correlation between δD and $\delta^{15}\text{N}$ over the last Termination to obtain a synthetic $\delta^{15}\text{N}$ curve when $\delta^{15}\text{N}$ data are missing. Yellow line: LIDIE output scenario when Datice is run with background LIDIE from $\delta^{15}\text{N}-\delta\text{D}$ scenario.

2 Variances profiles

Each background scenario is associated with a variance. If the variance is high, Datice is allowed to make a strong correction to the background scenario in the final chronology. On the opposite, if the variance is small, the final scenarios should be very close to the background ones.

We implemented variance profiles for accumulation rate, thinning function and LIDIE that have been slightly modified from their initial formulation in Lemieux-Dudon et al. (2010). They take into account the depth (variance increases with depth for some sites) as well as the deviation from the present-day conditions based on the accumulation rate values.

115 2.1 Thinning function

The variance on the thinning function is expressed as:

$$\sigma_T(z) = c_{T_1} + c_{T_2} \cdot \int^z \frac{D(z)}{T(z)} dz + c_{T_3} \cdot \frac{\sigma_{A,loc}}{\sigma_{A,loc}^{max}}$$

where c_{T_1} , c_{T_2} and c_{T_3} are user defined constant parameters (c_{T_2} equal $c \cdot 0.1/H$ where H is the maximum depth of the input and c a user defined constant), $T(z)$ is the thinning function, $D(z)$ the relative density, $\sigma_{A,loc}$ the local standard deviation of accumulation and $\sigma_{A,loc}^{max}$ the maximum standard deviation of accumulation. The last term was implemented in order to increase the thinning
 120 variances during transitions since it has been suggested that the mechanical properties of ice can be modified in these periods. The parameterization of this effect could be improved by modifying also the correlation length during these periods but would require additionnal tests for a correct parameterization. This last term is however of second order relatively to the depth dependence (Fig. 3b).

125 2.2 Accumulation rate

The variance is formulated as follows:

$$\sigma_A(z) = \sigma_{b,A} \cdot \frac{|A_0 - A|}{|A_0 - A|_{max}} \cdot \left(1 + c_{A_1} \frac{z}{z_{max}} \right)$$

with $\sigma_{b,A}$ being a reference standard deviation, A_0 is the mean Holocene accumulation rate, c_{A_1} is a constant parameter. The variance associated with the accumulation rate scenario thus increases when the background accumulation rate strongly deviates from the Holocene value. The reason for such a parameterization is that the reconstruction of accumulation rate from water isotopes through the exponential law is semi-empirical and its extrapolation far from the present-day conditions may be problematic.

In order to avoid too small variances, a threshold value, σ_m , is implemented for each ice core.

When σ_A is smaller than σ_m , then σ_A is recalculated as:

$$\sigma_A = \sigma_m \cdot \left(1 + c_{A_1} \frac{z}{z_{max}} \right)$$

where σ_m represents the minimum values, defined by user.

A dependence from upstream origin of the ice should be considered in the future.

2.3 LIDIE

The LIDIE variance is parameterized as:

$$\sigma_L(z) = \frac{\sigma_{b,L}}{\sigma_{b,A}} \cdot \frac{\sigma_A(z)}{1 + \frac{m_{A,loc}}{m_{A,loc}^{max}}}$$

130 with $m_{A,loc}$ being the local mean accumulation rate and $m_{A,loc}^{max}$ its maximum value over the length
of the core, $\sigma_{b,L}$ is a reference standard deviation. In this case, the variance on the LIDIE increases
with the variance on the accumulation rate, i.e. with the deviation from present-day conditions. This
is justified by the fact that we do not have a standardized way to link LIDIE to accumulation rate or
temperature (firnification model or $\delta^{15}\text{N}$ based estimate, see above).

135

An example of the resulting variances for the EDC core is presented on Fig. 2. The different coefficient values are given for each core in Table 2. The choice of variance remains necessary subjective but the following approach has been done:

- 140 – The depth dependence of the variances associated with accumulation rate and LIDIE has only
been considered for sites located on a slope and not on a dome. Hence, c_{A_1} has been assigned
a value of 1 for Vostok and EDML.
- A larger variance for LIDIE has been applied for sites where the firnification model and $\delta^{15}\text{N}$
approaches clearly disagree, i.e. for Vostok, EDML and EDC.
- 145 – A larger variance has been prescribed for EDML and Vostok thinning compared to EDC and
NorthGRIP because their location on a slope make the estimate of the background thinning
function from the glaciological model less certain.
- 150 – The thinning variance has been adjusted for TALDICE compared to EDC in order to avoid
dating inconsistencies produced by the glaciological background scenario of TALDICE thin-
ning. Indeed, the background scenarios obtained from glaciological model for TALDICE
gives an age model that is much too young with the δD optimum of MIS 5 occurring around
110 ka (Fig. 3a). This is in contradiction with available data suggesting that this optimum
should occur around 130 ka (Waelbroeck et al., 2008), with an uncertainty of several ka. It is
impossible that Termination II was only 110 ka old. Using the initial variance for the thinning
and accumulation rate of TALDICE produced a quite young Termination II because of the
155 influence of the TALDICE background scenario on the final chronology. We therefore had to
increase the variance associated with thinning at TALDICE (Fig. 3b).
- 160 – The variance on EDC and NorthGRIP thinning has been adjusted so that the new chronology
of MIS 5 and MIS 4 lies between the EDC3 and NorthGRIPmodelext chronologies. These two
initial chronologies were mostly derived from different glaciological constraints over this
particular period and there is no reason why one chronology should be preferred compared to
the other.

Many test of the variances assigned to the input scenarios were performed to evaluate the sensi-
tivity of the final solution to initial model conditions but cannot be detailed here.

Table 2. Coefficient values of the variance profiles for the different ice cores. With respect to LD2010, c_{T_1} has been lowered, c_{T_2} has been adjusted for each ice core and the term c_{T_3} added. The values of σ_b for accumulation rate and LIDIE have been kept from LD2010 except the value of $\sigma_{b,A}$ which has been increased for EDML.

	Thinning			Accu. rate		LIDIE
	c_{T_1}	c_{T_2}	c_{T_3}	$\sigma_{b,A}$	c_{A_1}	$\sigma_{b,C}$
Vostok	0.01	0.000084	0.15	0.6	1	0.7
EDC	0.01	0.000030	0.15	0.7	0	0.7
EDML	0.01	0.000078	0.15	0.5	1	0.6
TALDICE	0.01	0.000268	0.15	0.6	0	0.6
NGRIP	0.01	0.000016	0.05	0.6	0	0.6

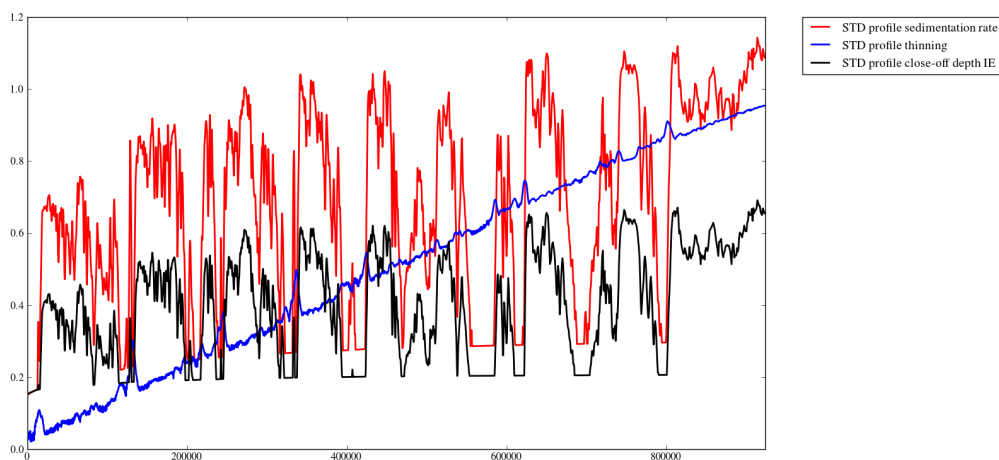


Fig. 2. Variances profiles of accumulation rate (red), LIDIE (black) and thinning function (blue) as function of age for EDC

3 Observations

165 The different markers included in Daticce are common for Veres et al. (2012) and Bazin et al. (2012).
 The database combines absolute ages, orbital markers, delta-depth markers and stratigraphic links
 in gas and ice phases to synchronize our five ice cores.

The AICC2012 chronology is also constrained back to 800 ka with the use of orbital markers when
 absolute markers are missing (Bazin et al., 2012).

170 Compared to the first Daticce application used to produce the chronology delivered by Lemieux-

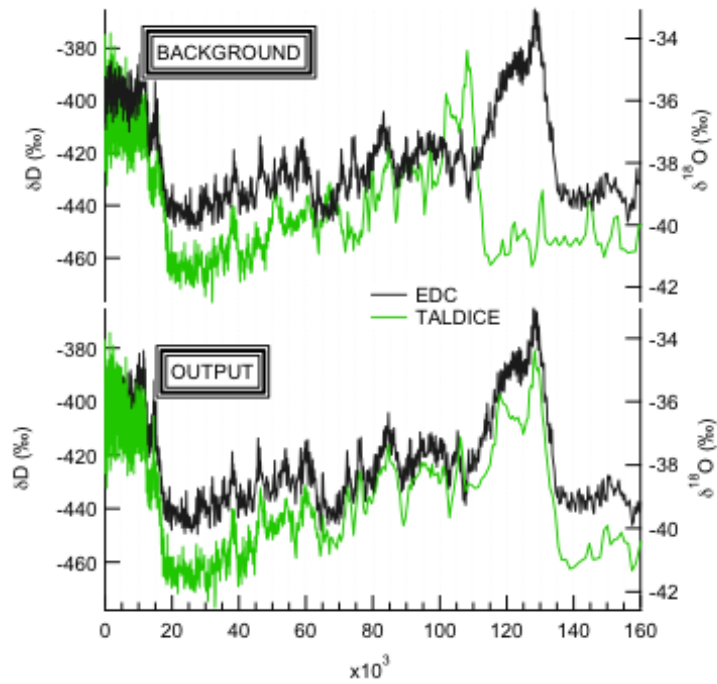


Fig. 3a. Upper panel: background chronologies from glaciological models for EDC (black) and TALDICE (green) Lower panel: output AICC2012 chronologies for EDC (black) and TALDICE (green)

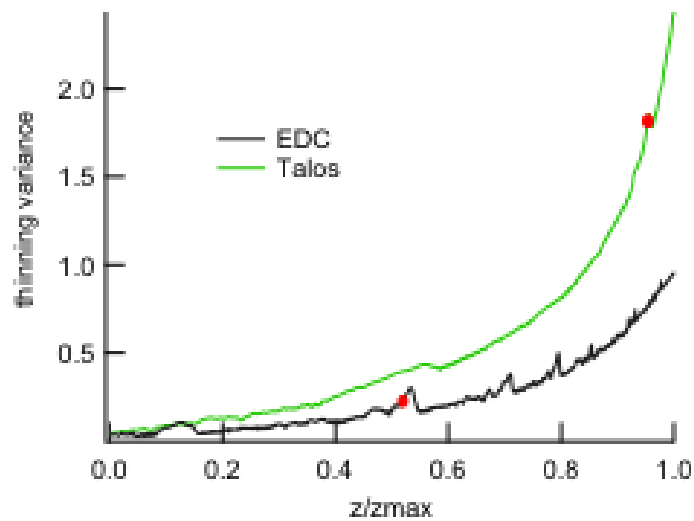


Fig. 3b. Thinning variances used for AICC2012 for EDC (black) and TALDICE (green). The red points correspond to the depth location of Termination II in the EDC and TALDICE ice cores.

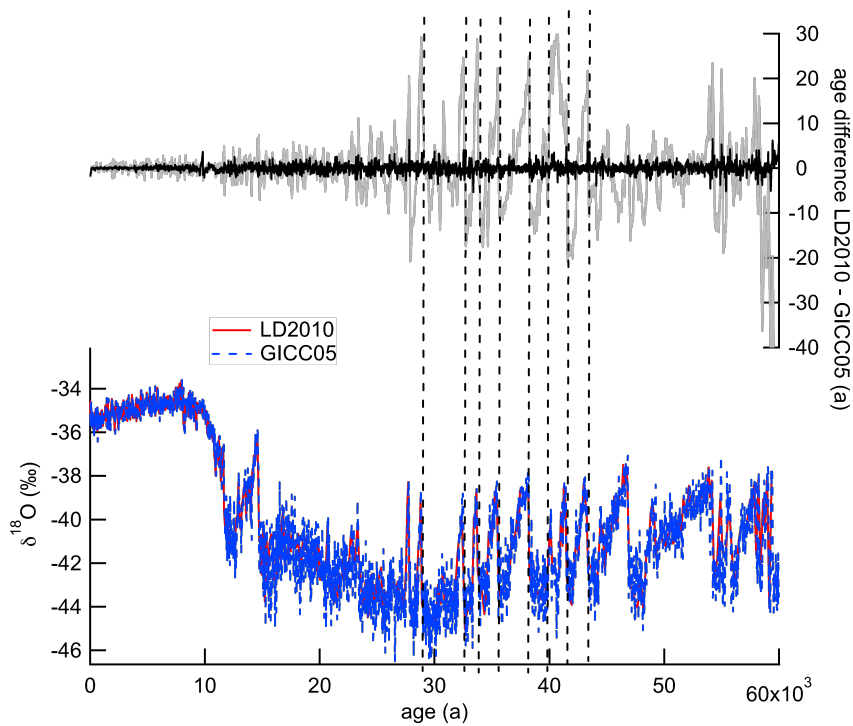


Fig. 4. NGRIP. Upper panel: difference between the LD2010 and GICC05 chronologies (grey); difference between the AICC2012 and GICC05 chronologies (black). Bottom panel: $\delta^{18}\text{O}$ records on the LD2010 and GICC05 chronologies.

Dudon et al. (2010), we wanted to suppress the climatic synchronization assumptions and avoid circular synchronisation markers. We have thus removed or modified the following absolute markers:

- Climatic orbital markers derived from δD insolation matching at Vostok (Parrenin et al., 2001).
- Speleothem point at 130.1 ka - see main text of Bazin et al. (2012)
- Air content orbital markers at Vostok and EDC - they have been replaced by the new table of orbital markers as explained in Bazin et al. (2012).
- All points derived by successive transfer between the cores (Parrenin et al., 2007)

3.1 Absolute age markers

The absolute ages described here are obtained from independent dating of events recorded in the cores. All absolute ages have been determined by argon dating with the standard of Kuiper et al. (2008) (Fish Canyon sanidine at 28.201 ± 0.046 Ma). Ages of the Laschamp event, Mount Moulton

eruption and Brunhes-Matuyama reversal have in some cases slightly changed from the published ages due to the re-calculation on the same standard.

185 **3.1.1 Vostok**

The absolute age markers for Vostok are deduced from ^{10}Be data. An age of 7.18 ± 0.10 ka at 178 m depth was assigned by comparison of the cosmogenic production of ^{10}Be and ^{14}C (Parrenin et al., 2001; Raisbeck et al., 1998).

190 The second age marker corresponds to the Laschamp event recorded at 601 m, associated with a revised age of 40.65 ± 0.95 ka (Raisbeck et al., 1987; Yiou et al., 1997; Singer et al., 2009).

3.1.2 EDC

EDC absolute ages are derived from ^{10}Be data and a tephra layer. The Laschamp event is recorded at 740 m and associated with an age of 40.65 ± 0.95 ka (Raisbeck et al., 2006; Singer et al., 2009).

195 The Mount Moulton eruption tephra layer is observed at 1265.1 m (Narcisi et al., 2006). Its age was first dated by Dunbar et al. (2008) on the Fish Canyon Tuff standard of (Renne et al., 1998), and when converted to the Fish Canyon sanidine standard of Kuiper et al. (2008) we finally obtain an absolute age of 93.2 ± 4.4 ka. The last two ages are associated with the Brunhes-Matuyama (B-M) reversal and its precursor, observed at 3165.5 m and 3183.5 m, and dated at 780.3 ka and 798.3 ka respectively (Raisbeck et al., 2006; Dreyfus et al., 2008). We decided to enlarge the uncertainty
200 associated with these ages (from 3.5 to 10 ka) because many different ages of the B-M reversal are found in the literature spanning over ± 10 ka (Channell et al., 2010; Coe et al., 2004; Camps et al., 2011; Mochizuki et al., 2011).

3.1.3 EDML

No absolute ages for the EDML ice core.

205 **3.1.4 TALDICE**

No absolute ages for the TALDICE ice core.

3.1.5 NGRIP

As in Lemieux-Dudon et al. (2010), we used absolute ages from GICC05 to force the model to respect the GICC05 chronology. Points were selected each 60 a over the last 60 ka (not listed, leading
210 to 990 points). We associated an uncertainty of maximum 50 years with the purpose of constraining AICC2012 tightly to GICC05, but in return did not use the absolute gas age markers of table 6 of (Lemieux-Dudon et al., 2010). Note that the background parameters of NGRIP (deduced from GICC05) and these markers are correlated, and this does not satisfy the hypothesis of independence

between background and data. However, this is the only practical way to constrain the final timescale
 215 tightly to GICC05 for the last 60 ka (Fig. 4).

3.2 Orbital age markers

The choice of the orbital markers and associated uncertainties is fully explained in Bazin et al.
 (2012).

3.3 Δ depth markers

220 Δ depth markers are only given for NorthGRIP over the last glacial period. They have been ob-
 tained by a depth comparison of the $\delta^{18}\text{O}_{\text{ice}}$ and air $\delta^{15}\text{N}$ profiles over the succession of Dansgaard-
 Oeschger events. Because of thermal isotopic fractionation, each step in $\delta^{18}\text{O}_{\text{ice}}$ corresponding to
 a rapid warming is recorded as a peak in $\delta^{15}\text{N}$ in the gas phase. The Δ depth markers have been
 measured as either the depth difference between the mid-slopes of $\delta^{18}\text{O}_{\text{ice}}$ and of $\delta^{15}\text{N}$ or as the
 225 depth difference between the peaks of $\delta^{18}\text{O}_{\text{ice}}$ and of $\delta^{15}\text{N}$. The uncertainty estimate is 2 m from
 the resolution of the measurements and the difference of Δ depth estimates (mid-slopes of peaks)
 (Table 3).

Table 3. List of Δ depth markers for NGRIP included in Datice

Depth(m)	Δ depth	Uncertainty (m)
2099.9	16.29	2
2123.6	15.8	2
2157.1	15.56	2
2218.2	15.7	2
2255.6	12.85	2
2345.2	11.74	2
2364.5	12.36	2
2419.31	11.6	2
2465.1	8.85	2
2506.9	8.16	1.5
2577.8	7.66	1.5
2685.1	7.15	2
2890.2	5.54	2
2895.8	4.44	1.5
2936.5	7.8	1.5

3.4 Gas stratigraphic links

The gas stratigraphic links comes from matching of CH₄ and δ¹⁸O_{atm} variations between ice cores following the published tie-points (references are provided in Table 4 of gas stratigraphic tie-points). δ¹⁵N data are used as markers of rapid warming in the NorthGRIP ice core when CH₄ data were not available (tie-points from Capron et al. (2010)). In some cases, the associated uncertainties had to be increased for obtaining the final chronology because of incoherencies in the final thinning, accumulation rate or LIDIE scenarios. A few tie-points had also to be removed because of similar incoherencies.

Table 4. Gas stratigraphic links between ice cores

Pairs	Nb. of points	Sources
Vostok-EDC	67	Lemieux-Dudon et al. (2010) Loulergue (2007) This study
Vostok-NGRIP	5	Landais et al. (2006)
EDC-EDML	64	Schilt et al. (2010) Loulergue et al. (2007) Loulergue (2007) This study
EDC-TALDICE	22	Buiron et al. (2011) Schüpbach et al. (2011)
EDC-NGRIP	6	Schilt et al. (2010)
EDML-TALDICE	13	Schüpbach et al. (2011)
EDML-NGRIP	45	Lemieux-Dudon et al. (2010) Schilt et al. (2010) Capron et al. (2010)
NGRIP-TALDICE	25	Buiron et al. (2011) (revised NGRIP depth)

3.5 Ice stratigraphic links

4 Application

Using all the previously cited inputs, the Datice tool is capable of calculating the best compromise between the background ages and the observations, using an inverse method (Lemieux-Dudon et al., 2010). On Fig. 5 we can visualize the improvement of the EDC chronology in the 1200 to 1340 m depth range. The background chronologies are represented by the dashed-black curve for the gas age and dashed-grey curve for the ice age. Different observations are represented with their uncertainties: some gas stratigraphic links (blue squares), some ice stratigraphic links (red squares) and absolute

Table 5. Ice stratigraphic links between ice cores

Pairs	Nb. of points	Sources
Vostok-EDC	104	Udisti et al. (2004) Parrenin et al. (2012b)
EDC-EDML	240	Ruth et al. (2007) Severi et al. (2007) This study
EDC-TALDICE	102	Severi et al. (2012)
EDC-NGRIP	2	Loulergue et al. (2007)
EDML-NGRIP	86	Vinther et al. (2012) Svensson et al. (2012)

ice ages (yellow triangles). After applying the inverse method, we finally obtain the blue and red
 245 curves corresponding to the best compromise between the background and observations for the gas
 (blue) and ice (red) chronologies. For example, we can see that at 1200 m depth the previous gas age
 was 80.5 ka (83.5 ka for the ice phase), now the new gas age is 81.5 ka (84.5 ka for the ice). Note that
 the blue and red curves necessarily fit perfectly the ice and gas stratigraphic markers (red and blue
 squares) because these stratigraphic markers are initially only given as depth constraints on each ice
 250 core, their respective ages are then calculated on the new chronology. On Fig. 5, the stratigraphic
 points have thus been placed corresponding to their calculated age on the new chronology. The error
 bars stand for the initial age uncertainties associated with these stratigraphic links.

5 Estimate of the uncertainty attached to the AICC2012 chronology

The estimate of the age uncertainty is done exactly the same way as in Lemieux-Dudon et al. (2010).
 We thus do not give it the details of the calculation given in the SOM of Lemieux-Dudon et al. (2010)
 but only the different terms implemented in this calculation.

Datice calculates an error covariance matrix denoted P , which is an estimate of the errors made
 on accumulation, thinning and LIDIE at each depth level and for each ice cores. The P matrix en-
 tirely depends on inputs of the dating problem: the B matrix storing the covariances of errors of
 the different background scenarios (accumulation, thinning, LIDIE); the R matrix storing the uncer-
 tainties associated with each data constraint (absolute, stratigraphic, orbital tie-points); and finally
 the H operator. H is the linearization of what is called the observation operator (data assimilation
 jargon). The observation operator, denoted h , predicts the data (absolute, stratigraphic, orbital tie-
 points) from a given scenario of accumulation, thinning and LIDIE. To illustrate this, the observation
 operator maps a vector $(a_1, \dots, a_n, t_1, \dots, t_n, c_1, \dots, c_n)$ whose components are accumulation, thinning

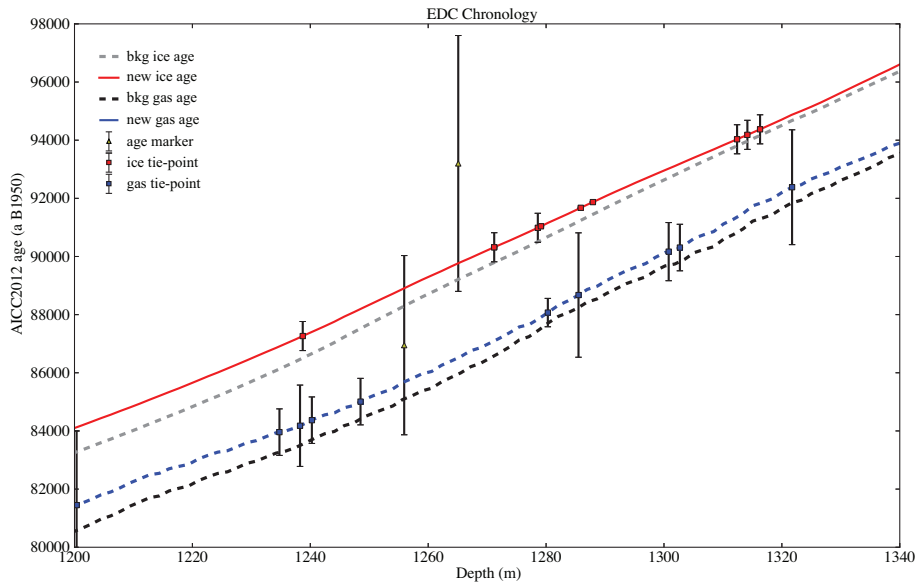


Fig. 5. Visualization of the Datice tool mechanism on the period 80 ka to 98 ka of the EDC ice core.

and LIDIE, into an age vector (h_1, \dots, h_N) that predicts the age at the age markers depths (z_1, \dots, z_N) . Under some assumptions, P expressed as:

$$P \simeq (B^{-1} + H^T R^{-1} H)^{-1}$$

The age error covariance matrix, C, is expressed as :

$$C \simeq H P H^T$$

C stores errors propagated from the background and observations variances and covariances. Near
 255 an absolute tie-point with a small associated uncertainty, the posterior error will thus be dominated
 by the observation error, while near a tie-point with a very large associated uncertainty, this error
 will mainly result from the variances (and covariances) associated with the background scenarios.
 Finally, one can note that the non-diagonal terms of the B matrix represents the error correlation of
 the background scenarios. The error correlation further increases the total error at each depth level
 260 because of errors at neighbour depth levels. The correlation lengths associated with these diagonal
 terms have an impact on the final error : large correlation lengths in depth ranges with several strong
 constraints will lead to very small final error on the chronology.

Figure 6 shows the calculated error by DATICE (standard deviation for ice age) for the 5 ice core
 265 AICC2012 chronologies. As expected, the error increases with depth because of : (1) the increase
 of variance associated with background scenario, (2) less numerous absolute, orbital or stratigraphic
 constraints with depth, (3) the increase of uncertainties attached to data constraints with depth, and

(4) the fact that error propagation applied to the ice age equation as a function of accumulation, and thinning cumulates the errors at each depth level. This is particularly visible for the NorthGRIP 270 chronology with the numerous absolute tie-points over the last 60 ka associated with an uncertainty of 1-50 years and much less data constraints prior to 60 ka.

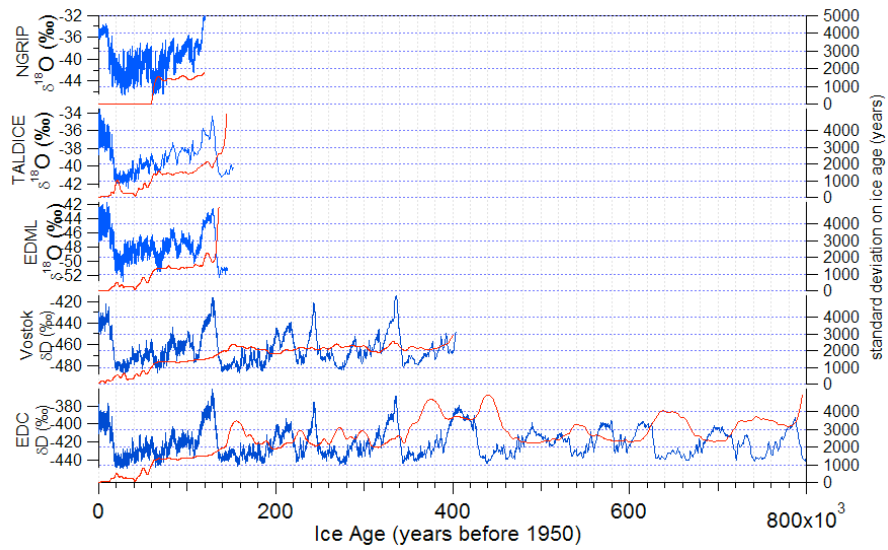


Fig. 6. $\delta^{18}O_{ice}$ records for the 5 ice cores on the AICC2012 chronology (blue) and standard deviation on ice ages for each ice core chronology (red).

References

- Andersen, K. K., Svensson, A., Johnsen, S. J., Rasmussen, S. O., Bigler, M., Röthlisberger, R., Ruth, U., Siggaard-Andersen, M.-L., Peder Steffensen, J., Dahl-Jensen, D., Vinther, B. M., and Clausen, H. B.: The
275 Greenland Ice Core Chronology 2005, 15 42 ka. Part 1: constructing the time scale, *Quaternary Science Reviews*, 25, 3246–3257, doi:10.1016/j.quascirev.2006.08.002, 2006.
- Bazin, L., Landais, A., Lemieux-Dudon, B., Toyé Mahamadou Kele, H., Veres, D., Parrenin, F., Martinerie, P., Ritz, C., Capron, E., Lipenkov, V., Loutre, M.-F., Raynaud, D., Vinther, B., Svensson, A., Rasmussen, S., Severi, M., Blunier, T., Leuenberger, M., Fischer, H., Masson-Delmotte, V., Chappellaz, J., and Wolff, E.:
280 An optimized multi-proxies, multi-site Antarctic ice and gas orbital chronology (AICC2012): 120-800 ka, *Climate of the Past*, This issue, 2012.
- Bender, M. L., Floch, G., Chappellaz, J., Suwa, M., Barnola, J.-M., Blunier, T., Dreyfus, G., Jouzel, J., and Parrenin, F.: Gas age-ice age differences and the chronology of the Vostok ice core, 0-100 ka, *Journal of Geophysical Research (Atmospheres)*, 111, D21115, doi:10.1029/2005JD006488, 2006.
- 285 Buiron, D., Chappellaz, J., Stenni, B., Frezzotti, M., Baumgartner, M., Capron, E., Landais, A., Lemieux-Dudon, B., Masson-Delmotte, V., Montagnat, M., Parrenin, F., and Schilt, A.: TALDICE-1 age scale of the Talos Dome deep ice core, East Antarctica, *Climate of the Past*, 7, 1–16, doi:10.5194/cp-7-1-2011, 2011.
- Camps, P., Singer, B. S., Carvallo, C., Goguitchaichvili, A., Fanjat, G., and Allen, B.: The Kamikatsura event and the Matuyama-Brunhes reversal recorded in lavas from Tjörnes Peninsula, northern Iceland, *Earth and
290 Planetary Science Letters*, 310, 33–44, doi:10.1016/j.epsl.2011.07.026, 2011.
- Capron, E., Landais, A., Lemieux-Dudon, B., Schilt, A., Masson-Delmotte, V., Buiron, D., Chappellaz, J., Dahl-Jensen, D., Johnsen, S., Leuenberger, M., Loulergue, L., and Oerter, H.: Synchronising EDML and NorthGRIP ice cores using $\delta^{18}\text{O}$ of atmospheric oxygen ($\delta^{18}\text{O}_{atm}$) and CH_4 measurements over MIS5 (80-123 kyr), *Quaternary Science Reviews*, 29, 222–234, doi:10.1016/j.quascirev.2009.07.014, 2010.
- 295 Capron, E., Landais, A., Buiron, D., Cauquoin, A., Chappellaz, J., Debret, M., Jouzel, J., Leuenberger, M., Martinerie, P., Masson-Delmotte, V., Mulvaney, R., Parrenin, F., and Prié, F.: Glacial-interglacial dynamics of Antarctic firns: comparison between simulations and ice core air-d15N measurements, *Climate of the Past*, This issue, 2012.
- Channell, J. E. T., Hodell, D. A., Singer, B. S., and Xuan, C.: Reconciling astrochronological and $^{40}\text{Ar}/^{39}\text{Ar}$ ages for the Matuyama-Brunhes boundary and late Matuyama Chron, *Geochemistry, Geophysics, Geosystems*, 11, Q0AA12, doi:10.1029/2010GC003203, 2010.
- 300 Coe, R. S., Singer, B. S., Pringle, M. S., and Zhao, X.: Matuyama-Brunhes reversal and Kamikatsura event on Maui: paleomagnetic directions, $^{40}\text{Ar}/^{39}\text{Ar}$ ages and implications, *Earth and Planetary Science Letters*, 222, 667–684, doi:10.1016/j.epsl.2004.03.003, 2004.
- 305 Dreyfus, G. B., Raisbeck, G. M., Parrenin, F., Jouzel, J., Guyodo, Y., Nomade, S., and Mazaud, A.: An ice core perspective on the age of the Matuyama-Brunhes boundary, *Earth and Planetary Science Letters*, 274, 151–156, doi:10.1016/j.epsl.2008.07.008, 2008.
- Dreyfus, G. B., Jouzel, J., Bender, M. L., Landais, A., Masson-Delmotte, V., and Leuenberger, M.: Firn processes and $\delta^{15}\text{N}$: potential for a gas-phase climate proxy, *Quaternary Science Reviews*, 29, 28 – 42, doi: 10.1016/j.quascirev.2009.10.012, 2010.
- 310 Dunbar, N. W., McIntosh, W. C., and Esser, R. P.: Physical setting and tephrochronology of the summit caldera

- ice record at Mount Moulton, West Antarctica, *Geological Society of America Bulletin*, 120, 796–812, doi: 10.1130/B26140.1, 2008.
- Goujon, C., Barnola, J.-M., and Ritz, C.: Modeling the densification of polar firn including heat diffusion: Application to close-off characteristics and gas isotopic fractionation for Antarctica and Greenland sites, *Journal of Geophysical Research (Atmospheres)*, 108, 4792, doi:10.1029/2002JD003319, 2003.
- Guillevic, M., Bazin, L., Landais, A., Masson-Delmotte, V., Blunier, T., Buchardt, S. L., Capron, E., Kindler, P., Leuenberger, M., Minster, B., Orsi, A., Prie, F., and Vinther, B. M.: Spatial gradients of temperature, accumulation and $\delta^{18}O$ -ice in Greenland over a series of Dansgaard-Oeschger events, *Climate of the Past*, This issue, 2012.
- Huber, C., Beyerle, U., Leuenberger, M., Schwander, J., Kipfer, R., Spahni, R., Severinghaus, J. P., and Weiler, K.: Evidence for molecular size dependent gas fractionation in firn air derived from noble gases, oxygen, and nitrogen measurements, *Earth and Planetary Science Letters*, 243, 61–73, doi:10.1016/j.epsl.2005.12.036, 2006.
- Huybrechts, P., Rybak, O., Pattyn, F., Ruth, U., and Steinhage, D.: Ice thinning, upstream advection, and non-climatic biases for the upper 89% of the EDML ice core from a nested model of the Antarctic ice sheet, *Climate of the Past Discussions*, 3, 693–727, 2007.
- Kuiper, K. F., Deino, A., Hilgen, F. J., Krijgsman, W., Renne, P. R., and Wijbrans, J. R.: Synchronizing Rock Clocks of Earth History, *Science*, 320, 500–, doi:10.1126/science.1154339, 2008.
- Landais, A., Barnola, J. M., Masson-Delmotte, V., Jouzel, J., Chappellaz, J., Caillon, N., Huber, C., Leuenberger, M., and Johnsen, S. J.: A continuous record of temperature evolution over a sequence of Dansgaard-Oeschger events during Marine Isotopic Stage 4 (76 to 62 kyr BP), *Geophys. Res. Lett.*, 31, L22211, doi: 10.1029/2004GL021193, 2004.
- Landais, A., Jouzel, J., Massondelmotte, V., and Caillon, N.: Large temperature variations over rapid climatic events in Greenland: a method based on air isotopic measurements, *Comptes Rendus Geoscience*, 337, 947–956, doi:10.1016/j.crte.2005.04.003, 2005.
- Landais, A., Waelbroeck, C., and Masson-Delmotte, V.: On the limits of Antarctic and marine climate records synchronization: Lag estimates during marine isotopic stages 5d and 5c, *Paleoceanography*, 21, PA1001, doi:10.1029/2005PA001171, 2006.
- Lemieux-Dudon, B., Blayo, E., Petit, J.-R., Waelbroeck, C., Svensson, A., Ritz, C., Barnola, J.-M., Narcisi, B. M., and Parrenin, F.: Consistent dating for Antarctic and Greenland ice cores, *Quaternary Science Reviews*, 29, 8–20, doi:10.1016/j.quascirev.2009.11.010, 2010.
- Loulergue, L.: Contraintes chronologiques et biogéochimiques grâce au méthane dans la glace naturelle : une application aux forages du projet EPICA, 2007, Ph.D. thesis, UJF, France, 2007.
- Loulergue, L., Parrenin, F., Blunier, T., Barnola, J.-M., Spahni, R., Schilt, A., Raisbeck, G., and Chappellaz, J.: New constraints on the gas age-ice age difference along the EPICA ice cores, 0-50 kyr, *Climate of the Past*, 3, 527–540, 2007.
- Mochizuki, N., Oda, H., Ishizuka, O., Yamazaki, T., and Tsunakawa, H.: Paleointensity variation across the Matuyama-Brunhes polarity transition: Observations from lavas at Punaruu Valley, Tahiti, *Journal of Geophysical Research (Solid Earth)*, 116, B06103, doi:10.1029/2010JB008093, 2011.
- Narcisi, B., Robert Petit, J., and Tiepolo, M.: A volcanic marker (92 ka) for dating deep east Antarctic ice cores,

- Quaternary Science Reviews, 25, 2682–2687, doi:10.1016/j.quascirev.2006.07.009, 2006.
- NorthGRIP Community Members: High-resolution record of Northern Hemisphere climate extending into the last interglacial period, *Nature*, 431, 147–151, doi:10.1038/nature02805, 2004.
- 355 Parrenin, F., Jouzel, J., Waelbroeck, C., Ritz, C., and Barnola, J.-M.: Dating the Vostok ice core by an inverse method, *J. Geophys. Res.*, 106, 31 837–31 852, doi:10.1029/2001JD900245, 2001.
- Parrenin, F., Barnola, J.-M., Beer, J., Blunier, T., Castellano, E., Chappellaz, J., Dreyfus, G., Fischer, H., Fujita, S., Jouzel, J., Kawamura, K., Lemieux-Dudon, B., Loulergue, L., Masson-Delmotte, V., Narcisi, B., Petit, J.-R., Raisbeck, G., Raynaud, D., Ruth, U., Schwander, J., Severi, M., Spahni, R., Steffensen, J. P., Svensson, A., Udisti, R., Waelbroeck, C., and Wolff, E.: The EDC3 chronology for the EPICA Dome C ice core, *Climate of the Past*, 3, 485–497, doi:10.5194/cp-3-485-2007, 2007.
- 360 Parrenin, F., Barker, S., Blunier, T., Chappellaz, J., Jouzel, J., Landais, A., Masson-Delmotte, V., Schwander, J., and Veres, D.: On the gas-ice depth difference (Δ depth) along the EPICA Dome C ice core, *Climate of the Past Discussions*, 8, 1089–1131, doi:10.5194/cpd-8-1089-2012, 2012a.
- 365 Parrenin, F., Petit, J.-R., Masson-Delmotte, V., Wolff, E., Basile-Doelsch, I., Jouzel, J., Lipenkov, V., Rasmussen, S. O., Schwander, J., Severi, M., Udisti, R., Veres, D., and Vinther, B. M.: Volcanic synchronisation between the EPICA Dome C and Vostok ice cores (Antarctica) 0–145 kyr BP, *Climate of the Past*, 8, 1031–1045, doi:10.5194/cp-8-1031-2012, 2012b.
- Raisbeck, G., Yiou, F., Bard, E., Dollfus, D., Jouzel, J., and Petit, J. R.: Absolute dating of the last 7000 years of the Vostok ice core using $10^B e$, *Mineral. Mag.*, 62A, 1228, 1998.
- 370 Raisbeck, G. M., Yiou, F., Bourles, D., Lorius, C., and Jouzel, J.: Evidence for two intervals of enhanced Be-10 deposition in Antarctic ice during the last glacial period, *Nature*, 326, 273–277, doi:10.1038/326273a0, 1987.
- Raisbeck, G. M., Yiou, F., Cattani, O., and Jouzel, J.: ^{10}Be evidence for the Matuyama-Brunhes geomagnetic reversal in the EPICA Dome C ice core, *Nature*, 444, 82–84, doi:10.1038/nature05266, 2006.
- 375 Rasmussen, S. O., Andersen, K. K., Svensson, A. M., Steffensen, J. P., Vinther, B. M., Clausen, H. B., Siggaard-Andersen, M.-L., Johnsen, S. J., Larsen, L. B., Dahl-Jensen, D., Bigler, M., Röthlisberger, R., Fischer, H., Goto-Azuma, K., Hansson, M. E., and Ruth, U.: A new Greenland ice core chronology for the last glacial termination, *Journal of Geophysical Research (Atmospheres)*, 111, D06102, doi:10.1029/2005JD006079, 2006.
- 380 Renne, P. R., Swisher, C. C., Deino, A. L., Karner, D. B., Owens, T. L., and DePaolo, D. J.: Intercalibration of standards, absolute ages and uncertainties in $^{40}\text{Ar}/^{39}\text{Ar}$ dating, *Chemical Geology*, 145, 117 – 152, doi: 10.1016/S0009-2541(97)00159-9, 1998.
- Ruth, U., Barnola, J.-M., Beer, J., Bigler, M., Blunier, T., Castellano, E., Fischer, H., Fundel, F., Huybrechts, P., Kaufmann, P., Kipfstuhl, S., Lambrecht, A., Morganti, A., Oerter, H., Parrenin, F., Rybak, O., Severi, M., Udisti, R., Wilhelms, F., and Wolff, E.: "EDML1": a chronology for the EPICA deep ice core from Dronning Maud Land, Antarctica, over the last 150 000 years, *Climate of the Past*, 3, 475–484, doi:10.5194/cp-3-475-2007, 2007.
- 385 Schilt, A., Baumgartner, M., Blunier, T., Schwander, J., Spahni, R., Fischer, H., and Stocker, T. F.: Glacial-interglacial and millennial-scale variations in the atmospheric nitrous oxide concentration during the last 390 800,000 years, *Quaternary Science Reviews*, 29, 182–192, doi:10.1016/j.quascirev.2009.03.011, 2010.

- Schüpbach, S., Federer, U., Bigler, M., Fischer, H., and Stocker, T. F.: A refined TALDICE-1a age scale from 55 to 112 ka before present for the Talos Dome ice core based on high-resolution methane measurements, *Climate of the Past*, 7, 1001–1009, doi:10.5194/cp-7-1001-2011, 2011.
- 395 Severi, M., Becagli, S., Castellano, E., Morganti, A., Traversi, R., Udisti, R., Ruth, U., Fischer, H., Huybrechts, P., Wolff, E., Parrenin, F., Kaufmann, P., Lambert, F., and Steffensen, J. P.: Synchronisation of the EDML and EDC ice cores for the last 52 kyr by volcanic signature matching, *Climate of the Past*, 3, 367–374, 2007.
- Severi, M., Udisti, R., Becagli, S., Stenni, B., and Traversi, R.: Volcanic synchronisation of the EPICA-DC and TALDICE ice cores for the last 42 kyr BP, *Climate of the Past*, 8, 509–517, doi:10.5194/cp-8-509-2012, 400 2012.
- Singer, B. S., Guillou, H., Jicha, B. R., Laj, C., Kissel, C., Beard, B. L., and Johnson, C. M.: $^{40}\text{Ar}/^{39}\text{Ar}$, K-Ar and ^{230}Th - ^{238}U dating of the Laschamp excursion: A radioisotopic tie-point for ice core and climate chronologies, *Earth and Planetary Science Letters*, 286, 80–88, doi:10.1016/j.epsl.2009.06.030, 2009.
- Sowers, T., Bender, M., Raynaud, D., and Korotkevich, Y. S.: $\delta^{15}\text{N}$ of N_2 in Air Trapped in Polar Ice: a Tracer 405 of Gas Transport in the Firn and a Possible Constraint on Ice Age-Gas Age Differences, *J. Geophys. Res.*, 97, 15 683–15 697, doi:10.1029/92JD01297, 1992.
- Svensson, A., Andersen, K. K., Bigler, M., Clausen, H. B., Dahl-Jensen, D., Davies, S. M., Johnsen, S. J., Muscheler, R., Parrenin, F., Rasmussen, S. O., Röthlisberger, R., Seierstad, I., Steffensen, J. P., and Vinther, B. M.: A 60 000 year Greenland stratigraphic ice core chronology, *Climate of the Past*, 4, 47–57, doi: 410 10.5194/cp-4-47-2008, 2008.
- Svensson, A., Bigler, M., Blunier, T., Clausen, H. B., Dahl-Jensen, D., Fischer, H., Fujita, S., Goto-Azuma, K., Johnsen, S. J., Kawamura, K., Kipfstuhl, S., Kohno, M., Parrenin, F., Popp, T., Rasmussen, S. O., Schwander, J., Seierstad, I., Severi, M., Steffensen, J. P., Udisti, R., Uemura, R., Vallelonga, P., Vinther, B. M., Wegner, A., Wilhelms, F., and Winstrup, M.: Direct linking of Greenland and Antarctic ice cores at the Toba eruption 415 (74 ka BP), *Climate of the Past*, This issue, 2012.
- Udisti, R., Becagli, S., Castellano, E., Delmonte, B., Jouzel, J., Petit, J. R., Schwander, J., Stenni, B., and Wolff, E. W.: Stratigraphic correlations between the European Project for Ice Coring in Antarctica (EPICA) Dome C and Vostok ice cores showing the relative variations of snow accumulation over the past 45 kyr, *Journal of Geophysical Research (Atmospheres)*, 109, D08101, doi:10.1029/2003JD004180, 2004.
- 420 Veres, D., Bazin, L., Landais, A., Lemieux-Dudon, B., Parrenin, F., Martinerie, P., Toyé Mahamadou Kele, H., Capron, E., Chappellaz, J., Rasmussen, S., Severi, M., Svensson, A., Vinther, B., and Wolff, E.: The Antarctic ice core chronology (AICC2012): an optimized multi-parameter and multi-site dating approach for the last 120 thousand years, *Climate of the Past*, This issue, 2012.
- Vinther, B., Clausen, H., Kipfstuhl, S., Fischer, H., Bigler, M., Oerter, H., Wegner, A., Wilhelms, F., Sevri, M., 425 Udisti, R., Beer, J., Steinhilber, F., Adolphi, F., Muschler, R., Rasmussen, S., Steffensen, J., and Svensson, A.: A stratigraphic Antarctic chronology covering the past 16700 years in the EPICA deep ice core from Dronning Maud Land, In prep, 2012.
- Vinther, B. M., Clausen, H. B., Johnsen, S. J., Rasmussen, S. O., Andersen, K. K., Buchardt, S. L., Dahl-Jensen, D., Seierstad, I. K., Siggaard-Andersen, M.-L., Steffensen, J. P., Svensson, A., Olsen, J., and Heinemeier, 430 J.: A synchronized dating of three Greenland ice cores throughout the Holocene, *Journal of Geophysical Research (Atmospheres)*, 111, D13102, doi:10.1029/2005JD006921, 2006.

- Waelbroeck, C., Frank, N., Jouzel, J., Parrenin, F., Masson-Delmotte, V., and Genty, D.: Transferring radiometric dating of the last interglacial sea level high stand to marine and ice core records, *Earth and Planetary Science Letters*, 265, 183–194, doi:10.1016/j.epsl.2007.10.006, 2008.
- 435 Wolff, E. W., Chappellaz, J., Blunier, T., Rasmussen, S. O., and Svensson, A.: Millennial-scale variability during the last glacial: The ice core record, *Quaternary Science Reviews*, 29, 2828–2838, doi:10.1016/j.quascirev.2009.10.013, 2010.
- Yiou, F., Raisbeck, G. M., Baumgartner, S., Beer, J., Hammer, C., Johnsen, S., Jouzel, J., Kubik, P. W., Lestringuez, J., Stievenard, M., Suter, M., and Yiou, P.: Beryllium 10 in the Greenland Ice Core Project ice
440 core at Summit, Greenland, *J. Geophys. Res.*, 102, 26 783–26 794, doi:10.1029/97JC01265, 1997.